Graphical abstract

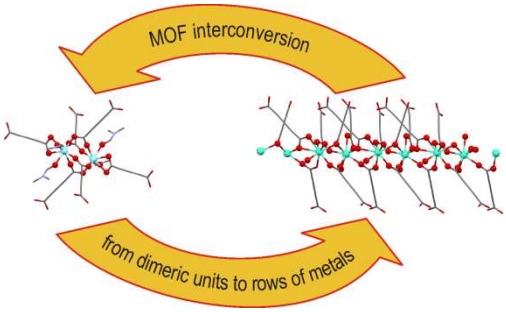

The MOF $\{[Gd_2(H_2L)_3(DMF)_4]\cdot 2DMF\}_n$ (H_4L = 2,5-dihydroxyterephtalic acid) has been cleanly converted into two different MOFs: $\{[Gd_2(H_2L)_3(H_2O)_6]\cdot 2H_2O\}_n$ and $\{[Gd_2(H_2L)(L)(H_2O)_5]\cdot 2H_2O\}_n$ with modifications in the MOF architecture that can be reverted.

Inorganica Chimica Acta

Interconversion of lanthanide-organic frameworks based on the anions of 2,5 dihydroxy terephtalic acid as connectors.

Jacopo De Bellis, Daniela Belli Dell'Amico, Gianluca Ciancaleoni, Luca Labella,* Fabio Marchetti, and Simona Samaritani

Dipartimento di Chimica e Chimica Industriale and CIRCC, Università di Pisa, via Giuseppe Moruzzi 13, I-56124

Highlights

Gadolinium-based metal organic frameworks were interconverted
Structural conversion from dinuclear units to rows of metals
MOF room temperature synthesis

Abstract

The dependence of the nature of the MOF from the synthetic conditions have been here faced studying the reaction of suitable lanthanide precursors with 2,5-dihydroxyterephtalic acid (H_4L). The interconversion between different lanthanide derivatives having $[H_2L]^{2-}$ and $[L]^{4-}$ as anionic spacers was observed. The known gadolinium coordination polymer (CP) $\{[Gd_2(H_2L)_3(DMF)_4]\cdot 2DMF\}_n$ (DMF = *N,N*-dimethylformamide), **1**, was prepared in DMF, either at 90 °C or also at room temperature, if assisted by a base diffusion. NMR monitoring for the synthesis of the analogous yttrium system (DMF, 90 °C) showed that the reaction progress relates with the formation of $NHMe_2$ by DMF decomposition. $\{[Y_2(H_2L)_3(DMF)_4]\cdot 2DMF\}_n$, **2**, isotypic with **1**, was obtained. The new structurally characterized CP $\{[Gd_2(H_2L)_3(H_2O)_6]\cdot 2H_2O\}_n$ **3**, has been prepared by initial thermal (T = 170 °C) desolvation of **1** in *vacuo* (P = $1\cdot 10^{-3}$ Torr), followed by a hydrothermal treatment. Interestingly, **3** reverted back to **1** by treatment in DMF at 90°C. Moreover **3** has been obtained starting from the metal nitrate and H_4L in hydrothermal conditions (140 °C; 12h) in the presence of the stoichiometric amount of NaOH. Long reaction times produced the intermediate formation of a mixture where it was possible to identify the new structurally characterized $\{[Gd_2(H_2L)_3]\cdot 2\ H_2O\}_n$, **4**, the known $\{[Gd_2(H_2L)_2(L)_{0.5}(H_2O)_3]\cdot 4H_2O\}_n$, **5** and $\{[Gd_2(H_2L)(L)(H_2O)_5]\cdot 2H_2O\}_n$, **6**, while at higher temperature (160 °C; 24h) the pure **6** was obtained. The observed transformations of **1** into **6** in H_2O involve H_4L elimination. On the other hand, it was found that the treatment of **6** in DMF in the presence of H_4L leads back to **1**. Single Crystal X Ray Diffraction (SCXRD) studies were carried out on the new species **2**, **3** and **4**.

Keywords: lanthanide; 2,5-dihydroxyterephtalic acid; MOF; interconversion.

1. Introduction

The design and the synthesis of new porous coordination polymers based on lanthanide centres are of great interest for their promising potential applications in several different fields as for example in gas storage and separation, fluorescence sensing, host-guest chemistry, and catalysis.[1]

Current interest is largely devoted to the construction of metal-organic frameworks (MOFs) through coordination of metal ions with multifunctional organic ligands as connectors.[2] The selection of a suitable connector is crucial for the self-assembly of a desired architecture. Among the different organic linkers, 2,5-dihydroxyterephthalic acid (Figure 1), H_4L, has been used to obtain several porous MOFs with *d* transition metal ions. It is characterized by two carboxylic groups rigidly located at an angle of 180° (1,4-benzenedicarboxylic acid functionalities) and two phenolic functionalities. The two carboxylic groups can be deprotonated more easily than the phenolic ones, yielding the 2,5-dihydroxyterephthalato anion $[H_2L]^{2-}$. By additional loss of the phenolic protons the tetra-anionic linker is formed $[L]^{4-}$.

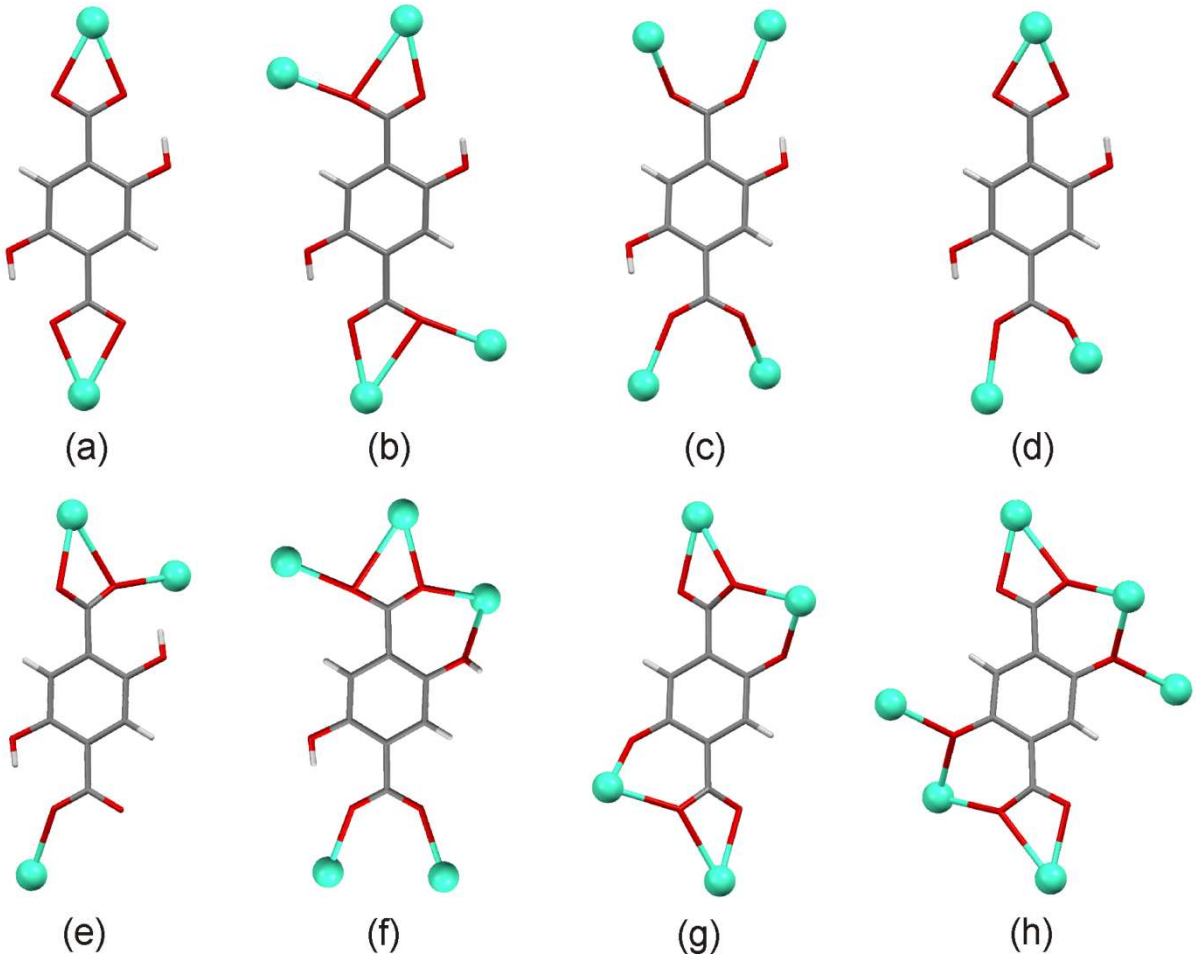

Figure 1. Different coordination modes of 2,5-dihydroxyterephtalato ligands (a-f $[H_2L]^{2-}$, g-h $[L]^{4-}$) in the frameworks described in this paper.

To preserve the phenolic functionalities in the hydrothermal synthetic conditions, initial protection and final deprotection in a post-synthetic modification[3] may be necessary. The majority of the *d* transition metals MOFs based on 2,5-dihydroxyterephthalic acid reported so far, contain the completely deprotonated tetra-anionic ligand.[4] Although high coordination numbers and flexible coordination geometries make more difficult to control the preparation of lanthanide complexes and less is reported on synthetic strategies for making lanthanide-based MOFs (Ln-MOFs),[5] a few

examples involving the 2,5-dihydroxyterephthalate ligand and lanthanides have been described.[6] It was interesting to find that phenolic functionalities could be retained without being protected in the synthetic conditions. Nevertheless, modifications in the course of the processes were observed, probably related to kinetic and thermodynamic parameters connected with the temperature and with the medium nature.

Many products can be considered kinetically driven lying on local thermodynamic minima, determined by factors such as solubility, solvent polarity, ionic strength of the medium, temperature, and pressure. Indeed, slight perturbations in synthetic parameters can afford many new MOF compounds.[7] The conversion of the kinetic MOF $\{[Tb_2(H_2L)_3(DMF)_4]\cdot 2DMF\}$ having free phenolic functionalities into the thermodynamic product $\{[Tb_2(H_2L)(L)(DMF)_2]\}_n$ containing also totally deprotonated ligands, was recently reported and discussed.[6e]

In the present paper, different MOFs have been prepared from the Gd(III)/H_4L system. The relevance of the synthesis conditions in defining the nature of the final products and the interconversion between different coordination polymers was evaluated changing the nature of the solvent and the temperature.

2. Experimental

2.1. Materials

Unless otherwise noted, all reagents were purchased from commercial sources and used without further purification. Hydrated gadolinium nitrate was prepared dissolving commercial metal oxide [Ln_2O_3 (Ln = Y, Gd; Aldrich)] in diluted nitric acid and evaporating the solution to dryness. The resulting solid residue was stored under nitrogen atmosphere[8] and its metal content was determined by complexometric titration.[9]

2.2. Instrumentation

^{1}H-, ^{13}C-NMR spectra were recorded with a Bruker ‘‘Avance DRX400’’ spectrometer. Chemical shifts were measured in ppm (δ) from TMS by residual solvent peaks for ^{1}H and ^{13}C. FTIR spectra in solid phase were recorded with a Perkin–Elmer ‘‘Spectrum One’’ spectrometer, equipped with an ATR accessory. Elemental analyses (C, H, N) were performed at Dipartimento di Chimica e Chimica Industriale, Università di Pisa.

Pulsed field Gradient Spin Echo NMR

^{1}H diffusion NMR measurements were performed by using the double-stimulated echo sequence with longitudinal eddy current delay at 298 K without spinning.[10] The dependence of the resonance

intensity (I) on a constant waiting time and on a varied gradient strength G is described by the following equation:

$$ln\frac{I}{I_0} = (\gamma\delta)^2 D_t \left(\Delta - \frac{\delta}{3}\right) G^2$$

where I is the intensity of the observed spin echo, I_0 the intensity of the spin echo in the absence of gradient, D_t the self-diffusion coefficient, Δ the delay between the midpoints of the gradients (0.2 s), δ the length of the gradient pulse (4 ms), and γ the magnetogyric ratio. The shape of the gradients was rectangular, and their strength G was varied during the experiments.

The self-diffusion coefficient, D_t, was estimated by evaluating the proportionality constant for a sample of HDO (5%) in D_2O (known diffusion coefficients in the range 274–318 K[11]) under the exact same conditions as the samples of interest. The solvent was taken as internal standard. The hydrodynamic volume of the species has been calculated from the experimental value of D_t through the procedure previously described.[12]

2.3. Synthesis

2.3.1. *Synthesis of {[Ln_2(H_2L)$_3$(DMF)$_4$] · 2DMF}$_n$ (Ln = Gd, 1; Ln = Y, 2) at 90° C*

Ln = Gd. $Gd(NO_3)_3 \cdot 5.5\ H_2O$ (1.34 g, 3.02 mmol) and H_4L (0.902 g, 4.55 mmol) were dissolved in 60 mL of DMF in a 500 mL Carius tube. After half an hour stirring, the yellow solution was heated at 90°C for 2 d. From the hot solution crystals started to form after a few hours. The very pale yellow, quasi colourless, product, represented mainly by single block crystals, was filtered and air dried. (1.79 g, 88.4 % yield). El. Anal.: Found: C, 36.7; H, 4.0; N, 6.4. Calc. for $\{[Gd_2(H_2L)_3(DMF)_4] \cdot 2DMF\}_n$ ($C_{42}H_{54}N_6Gd_2O_{24}$: C, 36.7; H, 4.1; N, 6.3%. ATR IR, ν_{max}/ cm^{-1} (4000-650 cm^{-1}): 3200-3010 (br), 2934 (vw), 1675 (vs), 1643 (s), 1610 (s), 1579 (m), 1495 (s), 1435 (vs), 1385 (vs), 1368 (vs), 1324 (m), 1307 (m), 1240 (vs), 1231 (vs), 1109 (m), 1094 (w), 1063 (w), 904 (w), 878 (w), 869 (m), 813 (s), 794 (vs), 783 (s), 730 (m), 679 (vs), 660 (m). The powder X-ray diffraction pattern was consistent with the single crystalline phase reported for **1**.

Ln = Y From $Y(NO_3)_3 \cdot 8\ H_2O$ (0.176 g, 0.542 mmol), H_4L (0.163 g, 0.823 mmol) and DMF (15 mL), following the same procedure described above, a pale yellow crystalline product was recovered (0.208 g, 63.7 %). El. Anal.: Found: C, 41.1; H.4.5; N, 6.8. Calc. for $\{[Y_2(H_2L)_3(DMF)_4] \cdot 2DMF\}_n$ ($C_{42}H_{54}N_6O_{24}Y_2$: C, 41.3; H, 4.5; N, 7.0%. ATR IR, ν_{max}/ cm^{-1} (4000-650 cm^{-1}): 3200-3020 (br), 2931 (vw), 1679 (vs), 1644 (s), 1622 (s), 1582 (s), 1496 (s), 1435 (vs), 1384 (vs), 1371 (s), 1307 (m), 1242 (s), 1230 (vs), 1109 (m), 1095 (m), 1063 (w), 914 (w), 903 (w), 871 (m), 813

(vs), 795 (vs), 784(s), 732 (m), 681 (s), 672 (s), 660 (m). Single crystals were selected for XRD studies.

*Room temperature syntheses of **1***

From $Gd(NO_3)_3 \cdot nH_2O$ by slow diffusion of NHR_2 (R = Bu, Me). A vial containing a solution of $Gd(NO_3)_3 \cdot 2.9\ H_2O$ (0.096 g, 0.24 mmol) and H_4L (0.079 g, 0.40 mmol) in DMF (10 mL) was introduced in a flask containing a solution of $[NH_2Bu_2][O_2CNBu_2]$ in heptane (10 mL, 0.594 M), under carbon dioxide atmosphere. After 1 month at room temperature large pale yellow crystals, formed in the vial, were filtered. (0.150 g, 93 % yield). Both IR spectrum and powder XRD pattern were consistent with those of **1**. In an analogous experiment carried out at room temperature with $[NH_2Me_2][O_2CNMe_2]$ in place of $[NH_2Bu_2][O_2CNBu_2]$, small-sized crystals of the same product were recovered in high yield.

From $[Gd(O_2CNBu_2)_3]$. $[Gd(O_2CNBu_2)_3]$ (see ESI; 0.229 g, 0.328 mmol), prepared following an already consolidated protocol,[13] was introduced into a 200 mL Carius tube containing H_4L (0.099 g, 0.50 mmol) and DMF (22 mL). Gas evolution was immediately observed with formation of an amorphous solid. A portion of the solid was identified as **1** through IR spectroscopy. Crystallization was favoured by heating the reaction mixture at 90°C for 12 h. The pale yellow crystalline solid was recovered by filtration and air-dried (0.173 g, 78.6 %). Elemental analysis, IR spectrum and PXRD pattern were in good agreement with those of **1**.

2.3.2. *Thermally assisted desolvation of 1 with formation of* $\{[Gd_2(H_2L)_3(DMF)_2]\}_n$, $\mathbf{1_{170}}$

A sample of **1** (1.00 g; 1.49 mmol of Gd) was first heated in vacuo ($1 \cdot 10^{-3}$ Torr) at 90°C for 4 d and then at 170°C for 3 d to yield 0.78 g of a pale yellow crystalline powder. Final recorded weight loss amounted to 22.0 % to original weight corresponding to the loss of approximately 2/3 DMF molecules per formula unit (calc. 21.8%). The product was stored under nitrogen atmosphere. El. Anal.: Found: C 33.0, H 2.5, N 3.0. Calc. for $\{[Gd_2(H_2L)_3(DMF)_2]\}_n$, $C_{30}H_{26}O_{20}N_2Gd_2$: C 33.3, H 2.5, N 2.7 %. ATR IR, solid (4000-650 cm^{-1}): 3490 (vw), 3200-3020 (w, br), 1673 (m), 1627 (m), 1587 (s), 1480 (m), 1447 (vs), 1434 (vs), 1401 (s), 1369 (vs), 1242 (s), 1222 (vs), 1179 (m), 1114 (m), 1060 (w), 905 (w), 867 (m), 810 (vs), 788 (vs), 730 (w), 680 (s) cm^{-1}. The product converted back into **1** after a treatment with DMF at 90°C (12 h) as revealed by IR spectrum and powder XRD pattern that were in good agreement with those of the original MOF.

2.3.3. *Conversion of 1_{170} into $\{[Gd_2(H_2L)_3(H_2O)_6] \cdot 2H_2O\}_n$, 3*

A sample of $\mathbf{1_{170}}$ (0.100 g, 0.19 mmol of Gd) was suspended in 7 mL of deionized water in a Carius tube (20 mL). The reaction mixture was heated at 120°C for 1 d. The pale yellow crystalline product was then recovered by filtration and dried by exposure to air. (0.052 g; 52 % yield). The

powder X-ray diffraction pattern well fitted the calculated pattern for the known $\{[Nd_2(H_2L)_3(H_2O)_6] \cdot 2H_2O\}_n$ [1]. ATR IR, solid (4000-650 cm^{-1}): 3480-2920 (br), 1680 (vw), 1637 (vw), 1564 (m), 1557 (m), 1516 (m), 1506 (m), 1496 (m), 1455 (s), 1435 (s), 1354 (m), 1316 (m), 1279 (m), 1245 (m), 1215 (s), 1123 (w), 1063 (vw), 998 (w), 902 (vw), 879 (m), 823 (m), 816 (m), 799 (vs), 778 (s), 740 (s), 707 (s), 655 (m) cm^{-1}. The product converted back to **1** after a treatment in DMF at 90°C (2 d) as characterized by IR spectrum and powder X-ray diffraction pattern.

2.3.4. ***Direct synthesis of 3***

The reaction mixture was obtained combining 6.0 mL of a 0.50 M aqueous solution of hydrated gadolinium nitrate (0.30 mmol Gd), 2,5-dihydroxyterephthalic acid (0.091 g, 0.46 mmol) and 9.00 mL of a 0.1 M standard aqueous solution of NaOH (0.900 mmol of NaOH) in a Parr Teflon-lined stainless-steel autoclave (30 mL). The vessel was sealed and transferred in an oven where it was heated to 140°C for 12 h. The brownish crystalline product, mainly single block crystals, was filtered and air dried. (0.127 g; 83 % yield). El. Anal.: Found: C 27.6, H 2.7. Calc. for $\{[Gd_2(H_2L)_3(H_2O)_6] \cdot 2H_2O\}_n$, $C_{12}H_{14}O_{13}Gd$: C 27.5, H 2.7 %. ATR IR, solid (4000-650 cm^{-1}): 3480-2920 (br), 1680 (vw), 1636 (vw), 1564 (m), 1558 (m), 1516 (m), 1506 (m), 1496 (m), 1455 (s), 1435 (s), 1354 (m), 1318 (m), 1279 (m), 1245 (m), 1215 (s), 1124 (w), 1063 (vw), 998 (w), 902 (vw), 879 (m), 823 (m), 816 (m), 799 (vs), 778 (s), 739 (s), 705 (s), 656 (m) cm^{-1}.

If no base was added, the reaction did not proceed and only the ligand recrystallization occurred.

For longer reaction times at 140 °C, a mixture of different crystalline phases was obtained. Single crystal XRD studies allowed to identify $\{[Gd_2(H_2L)_3] \cdot 2H_2O\}_n$, **4**, and powder XRD measurements afforded the recognition of $\{[Gd_2(H_2L)_2(L)_{0.5}(H_2O)_3] \cdot 4H_2O\}_n$, **5**, and $\{[Gd_2(H_2L)(L)(H_2O)_5] \cdot 2H_2O\}_n$, **6**.

2.3.5. ***Direct synthesis of 6***

$Gd(NO_3)_3 \cdot 4.1\ H_2O$ (0.247 g, 0.592 mmol), H_4L (0.118 g, 0.596 mmol) and 17.80 mL of a 0.1 M standard aqueous solution of NaOH (1.80 mmol NaOH) were introduced in a Teflon-lined stainless-steel autoclave. The vessel was sealed and transferred in an oven where it was heated at 160°C for 24 h. The green-yellow micro-crystalline product was filtered and air dried (0.217 g; 88.2 % yield). The powder X-ray diffraction pattern was in agreement with the calculated pattern of **6**.

2.3.6. *Conversion of* ***1*** *into* $\{[Gd_2(H_2L)(L)(H_2O)_5] \cdot 2H_2O\}_n$. ***6***

A sample of **1** (0.337 g, 0.251 mmol) was suspended into 12.5 mL of deionized water in a Parr Teflon lined stainless-steel autoclave (30 mL). The vessel was sealed and transferred in an oven where it was heated at 160°C for 24 h. The product green-yellow micro-crystalline solid was

recovered by filtration and dried by exposure to air. (0.162 g, 77.7 % yield). The powder X-ray diffraction pattern matched that of the pattern simulated from the single crystal structure of **6**.

2.**3.7.** ***Conversion of 6 into 1 by digestion in DMF at 90°C in presence of*** **H_4L**

A sample of **6** (0.048 g, 0.058 mmol) was suspended into 5 mL of an anhydrous solution of H_4L (0.023 g, 0.116 mmol) in DMF in a 20 mL Carius tube and the resulting mixture heated at 90°C for 16 h. The product was then recovered by filtration and dried by exposure to air. The overall yield amounted to 0.047 g of a colorless micro-crystalline solid. The powder X-ray diffraction pattern matched that of the pattern simulated from the single crystal structure of **1**. No reaction occurred in the absence of H_4L, the starting material being recovered intact according to PXRD.

2.4. Single-crystal X-ray Diffraction.

Crystals of **2, 3** and **4** were glued at the end of glass fibers. Diffractions were studied at room temperature by means of a Bruker SMART Breeze CCD diffractometer equipped with graphite monochromated Mo-$K\alpha$ radiation (λ = 0.71073 Å). The crystal data are listed in Table 1. Intensity data collections were carried out for all samples within the limits given in Table 1. All the structure solutions were found using the automated direct methods contained in SHELXS-97 program.[14] Hydrogen atoms were placed in calculated positions and were refined using a riding model. Two DMF molecules in the structure of **2** and one dihydroxyterephtalic acid in the structure of **4** are disordered. They were both refined as distributed on two limit positions fixing to one the total occupancy of the sites. The final reliability factors are listed in Table 1. Supplementary crystallographic data for this paper have been deposited with The Cambridge Crystallographic Data Centre and can be obtained free of charge from it. The deposition numbers for each compound are listed in Table 1.

Identification code	**2**	**3**	**4**
CCDC number	1885675	1885676	1885677
Empirical formula	$C_{21}H_{27}N_3O_{12}Y$	$C_{12}H_{14}O_{13}Gd$	$C_{12}H_9O_{11}Gd$
Formula weight	602.36	523.48	486.44
Crystal system	Triclinic	Triclinic	Monoclinic
Space group	$P\ \bar{1}$	$P\ \bar{1}$	$P\ 2_1/n$
a (Å)	10.5570(2)	8.0655(3)	6.5990(3)
b (Å)	10.9418(2)	9.8979(4)	16.0892(8)
c (Å)	12.9000(3)	10.6539(4)	12.9908(7)
α (°)	103.2030(10)	75.5030(10)	-
β (°)	111.1570(10)	74.668(2)	90.0240(10)
γ (°)	96.5110(10)	74.5590(10)	-
Volume (Å^3)	1321.09(5)	775.69(5)	1379.27(12)
Z	2	2	4
ρ_{calc} (g cm^{-3})	1.514	2.241	2.343
μ (mm^{-1})	2.272	4.349	4.872
F(000)	618	508	932
θ range (°)	2.9 to 29.6	3.0 to 35.3	3.4 to 34.1

Reflections collected	27037	25429	31025
Independent reflections	7352	6891	5424
Goodness-of-fit on F^2	1.047	1.137	1.188
Final R_1 $[I \geq 2\sigma(I)]$	0.0385	0.0149	0.0169
Final wR_2 $[I \geq 2\sigma(I)]$	0.0916	0.0372	0.0466
Final R_1 [all data]	0.0536	0.0159	0.0174
Final wR_2 [all data]	0.0967	0.0378	0.0468
Largest peak/hole (e Å^{-3})	0.945, –0.424	1.334, –0.490	0.782, –0. 894

Table 1. Crystal data and refinement summaries for **2**, **3** and **4**.

3. Results and discussion

Being aware that small differences can afford different outcomes in the synthesis of lanthanide MOFs, it appeared interesting to investigate the reaction of a gadolinium precursor with H_4L in various conditions. At the beginning, suitable conditions to guarantee a good reproducibility in high yield for a large scale synthesis of $\{[Gd_2(H_2L)_3(DMF)_4] \cdot 2DMF\}_n$, **1**,[6a] have been established. In anhydrous DMF, the reaction between hydrated gadolinium nitrate and H_4L, in the correct molar ratio, carried out at about 90 °C, afforded well shaped pale yellow crystals separating out of the solution after a few hours with achievement of excellent yields in 48 h (about 1.8 g and 90 % yield). Therefore, the product appeared to have a poor solubility in DMF also at high temperature (90°C). The powder X-ray diffraction pattern was consistent with the presence of the single, already reported crystalline phase for the isotypical species $\{[Ln_2(H_2L)_3(DMF)_4] \cdot 2DMF\}_n$. (Ln = La, Pr, Nd, Sm, Gd, Tb, Er).[6]

In the same conditions, the reaction between yttrium nitrate and H_4L produced the highly crystalline product $\{[Y_2(H_2L)_3(DMF)_4] \cdot 2DMF\}_n$, **2**, showing a PXRD pattern and a FTIR spectrum practically identical to the ones of **1** (Figure S1 and S2). Consistently a single crystal X-ray diffraction study showed that this compound is isostructural with the gadolinium derivative. Within this paper, all structural frameworks have been presented using a simplified representation of the 2,5-dihydroxyterephthalato groups, Figure 2, in order to make them more intelligible.

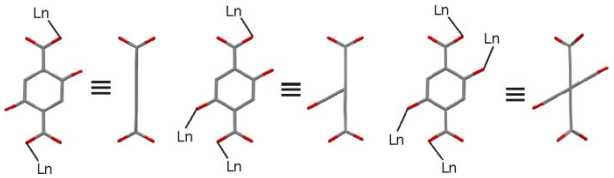

Figure 2. Simplified representation (respectively a-e; f; and g-h coordination modes) of the 2,5-dihydroxyterephthalato ligand.

The structure of **2** is based on dimeric units where two metal ions, related by an inversion centre, are bridged by four carboxylate groups belonging to four spacers (Figure 3).

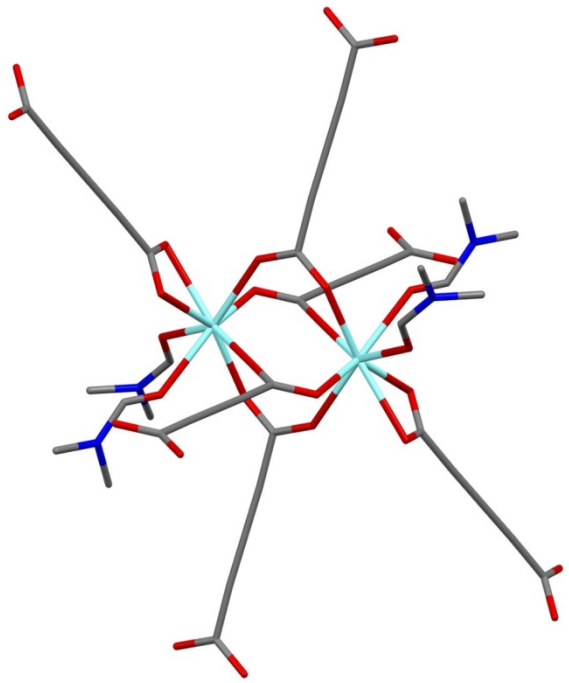

Figure 3. Couple of yttrium atoms in the structure of **2**. Color of the sticks is gray for C, red for O, blue for N and turquoise for Y.

The coordination around yttrium involves six oxygen atoms from five different H_2L^{2-} anions, and two oxygen atoms from two DMF ligands, in an approximately square antiprismatic geometry. Coordination modes 1a, and 1c for the H_2L^{2-} ligands have been observed. Y–O bond distances are ranging from 2.267 to 2.507 Å. For the gadolinium derivative, two of the four bridging carboxylate groups are described as terdentate (1b coordination mode) by some authors[6a] extending thus to 9 the coordination number of the metal. The additional Gd–O distance is about 2.80 Å long, considerably longer than all the other Ln–O distances (from 2.31 to 2.61 Å) and involving an oxygen atom kept in place by two other bonds. For the yttrium compound the analogous Y–O distance is at 3.085 Å, too long to be considered a bond distance. The yttrium compound has 3D frameworks with 1D open channels with an almost square cross-section of 10.95 × 9.20 $Å^2$ running in the [1 0 1] direction that accommodate the coordinated and guest DMF molecules (Figure 4). Half of the coordinated DMF and all DMF hosted in the channels (omitted in the figures) are disordered.

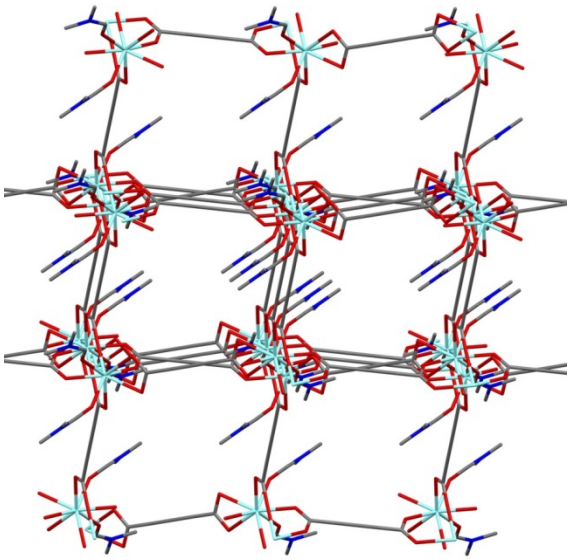

Figure 4. Framework of **2** projected approximately in the [1 0 1] direction. Hydogen atoms and guest DMF molecules have been omitted and H_2L^{2-} ligands have been represented in a simplified way for clarity.

The synthesis of the diamagnetic yttrium derivative offered the chance to monitor the reaction by NMR techniques. The analysis of the DMF solution during heating could give pieces of information about the MOF formation pathway, as for instance the identification of an initial molecular moiety able to progressively grow according to a modular design, with the idea to check if initial intermediates may have a suitable solubility in DMF to be detected. The spectrum of a solution of H_4L in d_7-DMF showed (besides the signals due to the residual non-deuterated solvent) a signal at 7.42 ppm due to the aromatic protons, a broad signal at 11 ppm attributable to the COOH and to the phenolic protons in fast exchange and a broad signal at 3.6 ppm due to water traces. Two samples containing $Y(NO_3)_3 \cdot n(H_2O)$ and H_4L in d_7-DMF were prepared; one was maintained at room temperature and the other was warmed up to 90 °C. At room temperature, the signal due to the H_4L aromatic protons essentially maintained the same position (7.40 ppm) while the signals at 3.6 and 11.0 coalesced in an unique broad signal at 7.3 ppm, the phenomenon being related to the increase of water concentration due to the introduction of a hydrated yttrium salt causing a faster proton exchange. After a prolonged warming of the mixture at 50°C, or also at 70°C, no variations were detected, while a new broad signal, due to a new species (**A**), appeared at 8.6 ppm after warming at 90 °C. Its intensity increased with time and a comparison with the spectrum of a d_7-DMF solution of $[NH_2Me_2]Cl$ allowed to attribute it to the NH_2 protons of the cation $[d_6\text{-}NH_2Me_2]^+$. As a confirmation, the diffusion coefficient (D_t) of **A** (Supporting Information) was measured through the Pulsed field Gradient Spin Echo (PGSE) NMR experiment, giving a value of $10.4 \cdot 10^{-9}$ m^2/s, comparable with the value obtained for the d_7-DMF solution of pure $[NH_2Me_2]Cl$, $9.8 \cdot 10^{-9}$ m^2/s.

Indeed, it is widely reported that DMF can be more than a solvent becoming the source of various key intermediates mediating reactions, as for instance CO and $NHMe_2$.[15] In the presented syntheses, the assistance of a base ($NHMe_2$) can be crucial as it buffers the production of HNO_3.(Eqs 1-3). Also the D_t of the ligand (7.4 ppm) has been monitored, but it remained constant at $5.8 \cdot 10^{-9}$ m^2/s throughout the entire treatment. Such a value is slightly smaller than that of the free ligand H_4L ($6.2 \cdot 10^{-9}$ m^2/s), ruling out the presence in solution of large aggregates, if not at very low concentrations. Similarly, the ^{13}C NMR spectra of H_4L did not show significant modification, either adding the yttrium nitrate and after prolonged warming (Supporting Information).

For the sample maintained at room temperature no modifications of the spectra were observed in the same time span.

$$2\ Ln(NO_3)_3 + 3\ H_4L + 6\ DMF \rightarrow 1/n\ \{[Ln_2(H_2L)_3(DMF)_4] \cdot 2DMF\}_n + 6\ HNO_3 \quad (1)$$

$$Me_2NC(O)H \rightarrow NHMe_2 + CO \quad (2)$$

$$NHMe_2 + HNO_3 \rightarrow [NH_2Me_2][NO_3] \quad (3)$$

In the self-assembly synthesis of a MOF, temperature may play an important role for both kinetic or thermodynamic aspects.[16] Phases unstable at high temperature or requiring a high activation energy to proceed to more stable assemblages, could be intercepted at low temperature. A room temperature reaction has been studied starting from gadolinium nitrate and H_4L in DMF to check the progress of the reaction and the nature of the products. As the decomposition of DMF is not observed at room temperature, a base was added to favor the reaction. Gadolinium nitrate and H_4L in molar ratio 2:3 reacted in DMF with the assistance of a quite slow diffusion of $NHBu_2$, originating from a solution of $[NH_2Bu_2][O_2CNBu_2]$ that was obtained by treatment of $NHBu_2$ with CO_2 in heptane (Eq 4).

$$2\ NHBu_2 + CO_2 \rightleftharpoons [NH_2Bu_2][O_2CNBu_2] \quad (4)$$

After a few days large crystals of the known phase of $\{[Gd_2(H_2L)_3(DMF)_4] \cdot 2DMF\}_n$, **1** started to form, with a yield higher than 90 % in one month. The product was characterized by elemental analysis, FTIR and PXRD. A similar experiment carried out with $[NH_2Me_2][O_2CNMe_2]$ as source of the base ($NHMe_2$) produced more quickly (98 % yield in 10 d) a microcrystalline powder of the same product. A similar result was obtained by slow diffusion of $NHBu_2$ from a solution of the amine in heptane (microcrystalline powder, about 78 % yield in 15 d). Taking into account that the reaction was promoted by a base, we reckoned that the base could be generated in situ starting from a gadolinium precursor able to release amine in the course of the process. The *N,N*-dibutylcarbamato complex of gadolinium, $[Gd(O_2CNBu_2)_3]$, was then prepared following an already consolidated protocol developed for some other lanthanides.[13] Metal carbamato complexes,

of general formula $[M(O_2CNR_2)_n]$, undergo protolysis by protic reagents HA with formation of $[MA_n]$, evolution of CO_2 and release of the amine, NHR_2 (Eq 5).[17]

$$[M(O_2CNR_2)_n] + n\,HA \rightarrow [MA_n] + n\,CO_2 + n\,NHR_2 \quad (5)$$

The reaction of $[Gd(O_2CNBu_2)_3]$ with H_4L proceeded quickly at room temperature in DMF with gas evolution and precipitation of an amorphous solid. The FTIR of the solid was identical to the one of $\{[Gd_2(H_2L)_3(DMF)_4] \cdot 2DMF\}_n$. The treatment of the powder at 90 °C in the liquor mother promoted the crystallization of the product that was characterized by elemental analysis, FTIR and powder PXRD (Figure S3 and S4).

In these processes, carried out in DMF containing traces or minor amounts of H_2O, essentially deriving from the hydrated gadolinium nitrate used as precursor, the temperature variation in the range 25-90 °C does not appear to affect the nature (composition and crystalline phase) of the product. Considering that the synthesis of **1** in DMF was previously described at 150°C,[6a] the temperature range of stability of **1** in DMF appears to be even larger. Moreover, although the introduction of a base does not produce variations in the chemical composition, nevertheless, the procedure influences the crystal dimensions, a slower base addition corresponding to the growth of larger crystals.

To control the modification of $\{[Gd_2(H_2L)_3(DMF)_4] \cdot 2DMF\}_n$ with the temperature in the solid state the product was treated at 170 °C under vacuum for 72 h and a weight loss corresponding to the removal of approximately 4 DMF molecules per formula unit was observed consistent with the removal of the DMF hosted in the MOF channels and of half of the coordinated one. Elemental analysis on the resulting product, $\mathbf{1_{170}}$, can help us to assign the composition $[Gd_2(H_2L)_3(DMF)_2]_n$. The PXRD pattern (Figure S5) is consistent with a few structural modifications. Structural details have been precluded by the change in the crystalline habit of the sample: large dimension single crystals turned into a microcrystalline powder even for longer treatment at lower temperatures. The infrared spectrum confirms an uncomplete removal of coordinated DMF (Figure S6). No deprotonation of $[H_2L]^{2-}$ to $[L]^{4-}$ with concomitant loss of H_4L occurred in the course of the thermal treatment of the solid sample of **1** (Figure S6). Interestingly, the treatment of $\mathbf{1_{170}}$ in DMF at 90°C for 12 h afforded **1** as confirmed by IR spectroscopy and powder XRD pattern control.

On the other hand, when $\mathbf{1_{170}}$ was suspended in deionized water and heated at 120°C a pale yellow crystalline product was obtained, **3**. The formula $\{[Gd_2(H_2L)_3(H_2O)_6] \cdot 2H_2O\}_n$ was assigned to the product, as its PXRD pattern corresponded to the calculated one of $\{[Nd_2(H_2L)_3(H_2O)_6] \cdot 2H_2O\}_n$ [6d] (Figure S7).

The product composition was confirmed by elemental analysis and infrared spectroscopy (Figure S8) and by comparison with an authentic sample obtained by a direct synthesis of **3** from hydrated gadolinium nitrate. The process was carried out in water, in hydrothermal conditions (140 °C, 12 h), in the presence of the stoichiometric amount of NaOH to favor the reaction progress through HNO_3 neutralization. The reaction did not proceed in absence of the base.

$$2\ Gd(NO_3)_3 + 3\ H_4L + 8\ H_2O \rightarrow 1/n\ \{[Gd_2(H_2L)_3(H_2O)_6]\cdot 2H_2O\}_n + 6\ HNO_3 \quad (6)$$

3

The crystal structure of **3** is shown in Figure 5. The framework consists of stepped 2D layers held together in the third dimension by an extensive net of hydrogen bonds involving the interlayer water molecules not represented in the Figure. The single layer appears in the side and top view in Figure 6. It consists of a quadrangular knit network whose nodes are the centrosymmetric dimeric units $Ln_2(H_2L)_6(H_2O)_4$. The lanthanide centre is nine-coordinated (six carboxylate oxygen atoms from four $[H_2L]^{2-}$ ligands and three oxygen atoms from water molecules) with Gd–O distances ranging between 2.347 and 2.726 Å. As clearly shown in the top view of the layer, there are two coordination modes of the spacers $[H_2L]^{2-}$ (Figure 1, a and e modes). Parallel ligands in the 1d coordination mode show π-π stacking. The hydroxyl groups of connectors are not involved in coordination but are engaged in hydrogen bonding.

3 reverted back into **1** if treated in DMF at 90°C as verified by IR and PXRD measurements.

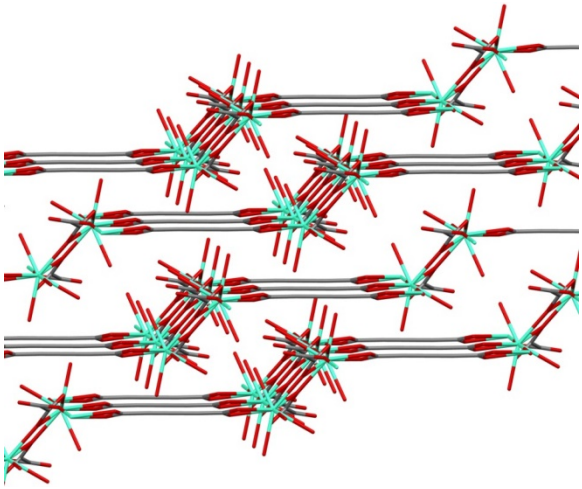

Figure 5. Stepped layers in the structure of **3** projected approximately in the [$\bar{1}$ 0 1] direction. Hydrogen atoms and interlayer water molecules are omitted for clarity.

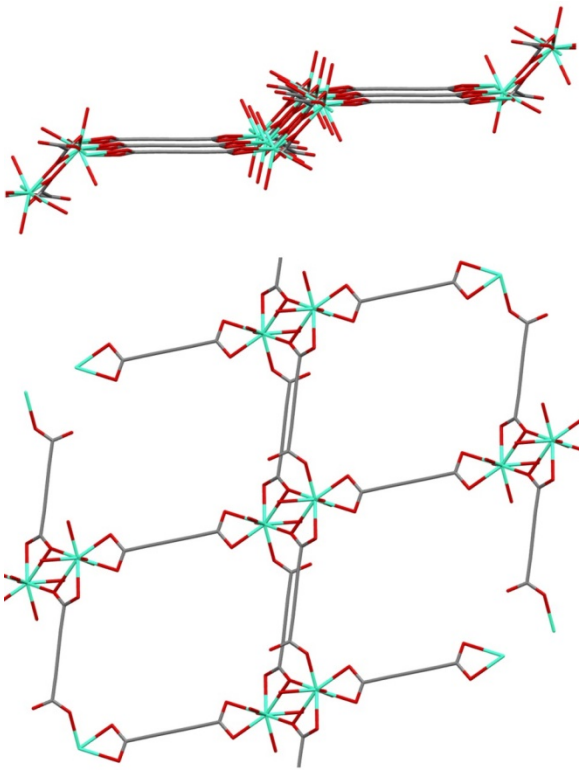

Figure 6. Side and top view of a single layer in the structure of **3**.

It is interesting to note that in water for longer reaction times (more than 1d at 140°C), starting from the hydrated gadolinium nitrate and H_4L, in the presence of the stoichiometric amount of NaOH, a mixture of different crystalline phases was obtained containing the known products $\{[Gd_2(H_2L)_2(L)_{0,5}(H_2O)_3] \cdot 4H_2O\}_n$, **5**, and $\{[Gd_2(L)(H_2L)(H_2O)_5] \cdot 2H_2O\}_n$, **6**, corresponding to progressive further deprotonation of the ligand with consequent variation of the connector/M molar ratio from, 1.5 in **3** to 1.25 in **5** and finally to 1 in **6** (Figure 7). In the solid mixture also the new derivative $\{[Gd_2(H_2L)_3] \cdot 2H_2O\}_n$, **4**, was obtained and characterized by single crystal diffractometric methods, as discussed below. It is worth to mention that also other unidentified microcrystalline phases were present in the mixtures and that, despite several attempts, their identification was not possible. Nevertheless, when the reaction was carried out at 160°C for 24 h, the powder X-ray diffraction of the green-yellow microcrystalline product was consistent with the presence of a single phase showing a pattern in good agreement with that calculated from the single crystal structure of **6**.

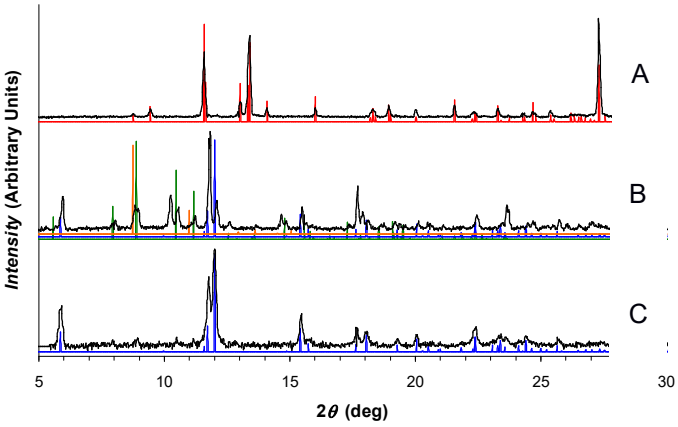

Figure 7. Powder-XRD of the solid obtained starting from the hydrated gadolinium nitrate and H_4L in a molar ratio 1 to 1.5, in the presence of the stoichiometric amount of NaOH after 12 h at 140 °C (A) after 2d at 140 °C (B) or after 1 d at 160 °C (C). Calculated pattern for **3** in red, for **4** in orange, for **5** in green and for **6** in blue.

It is interesting to note that in the previously reported[6d] crystal structure of **5**, centrosymmetric dimeric moieties as observed in **2** and in **3** are no more present. Instead, **5** contains an asymmetric unit made by two independent eight-coordinated Gd(III) ions making infinite rows of metals ···O1–Gd1–O2–Gd2–O3···with O1, O2 and O3 phenolic donor atoms of a $[L]^{4-}$ ligand (Figure 8). These rows run along the *a* direction, which is also the direction of the largest extension of the prismatic crystals. The dianionic $[H_2L]^{2-}$ ligands display two different coordination modes 1c and 1d (Figure 1) while the tetraanionic $[L]^{4-}$ ligand exhibits the coordination mode 1h. Each row is connected to four neighboring rows through the bridging spacers in a framework shown in Figure 8 reported here together with an image of the whole network (Figure 9) for comparison purposes with the other compounds discussed in this work.

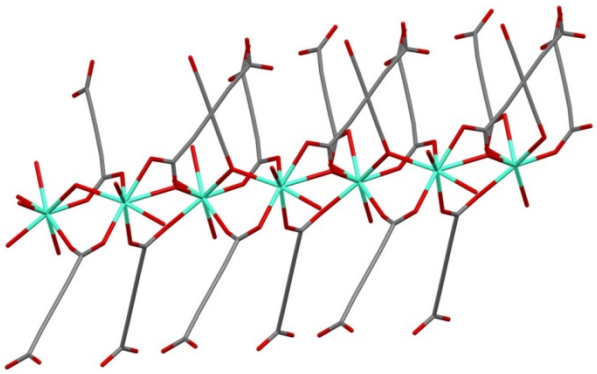

Figure 8. Row of metals running in the *a* direction in the structure of **5**. View in the *b* direction.

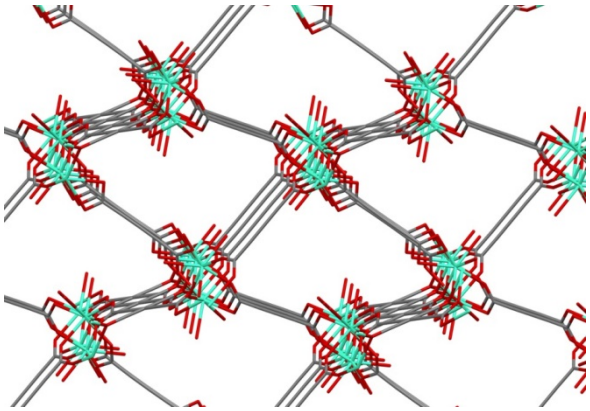

Figure 9. View of the 3D framework in the structure of **5** projected in the *a* direction.

Also in the already reported[6c] bilayered structure of **6** infinite rows of metals are determined by the presence of fully deprotonated spacers. Here two independent gadolinium atoms in the asymmetric unit with only two coordination modes 1c and 1g (Figure 1) of the ligand are present. Tetraanionic L^{4-} ligands chelating two Gd1 and two Gd2 centres form a 2D sheet pillared by the H_2L^{2-} ligands to another analogous sheet to produce the bilayer shown in Figure 10. The structure is characterized by the presence of the L^{4-} ligand on the opposite sides of the metal rows in a planar disposition as can be seen in Figure 11. The layered nature of the crystal structure is reflected in the habit of the crystals which are laminar or tabular flattened on the face {0 1 0}.

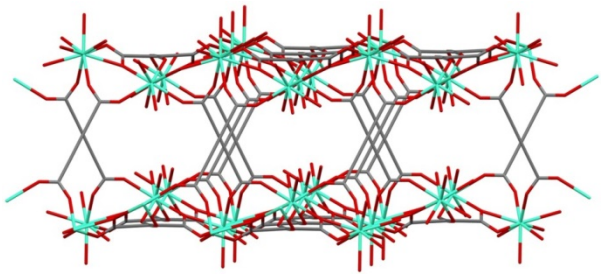

Figure 10. Pillared bilayer in the structure of **6** projected in the *c* direction.

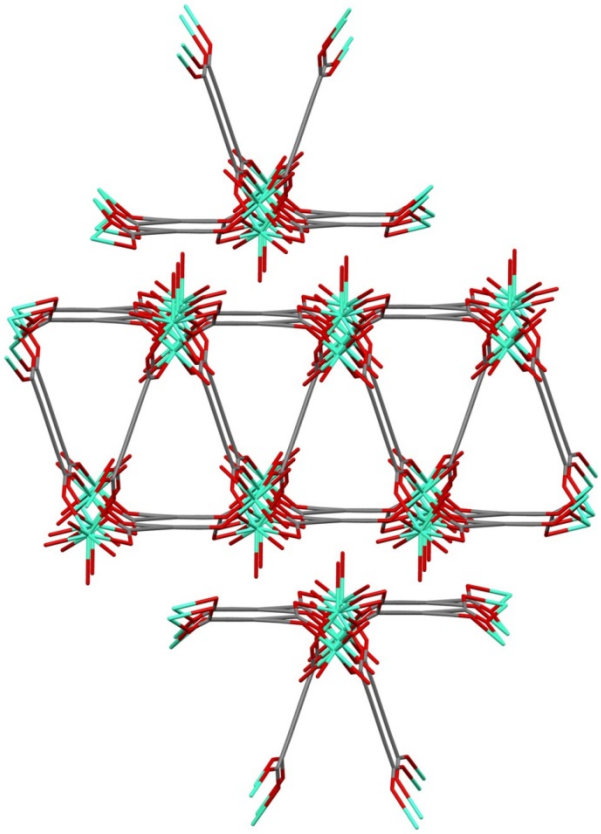

Figure 11. View of the layer structure of **6** projected in the *a* direction.

The structural types we met in this work show a transition from dimeric units to rows of metals. In **2** (as in **1**) and in **3** we find the connectors in their dianionic state, H_2L^{2-}, involving only their carboxylic moieties in the coordination to metals. The nodes are dinuclear with the two lanthanide centres bridged by four carboxylates of four different H_2L^{2-} ligands. The dinuclear units are in turn interconnected by the divergent ligands.

In **5** and **6** we can notice the involvement of the phenolic functionalities in the ligand coordination to metal affording a disposition in which the L^{4-} ligand bridges rows of metals. Progressive involvement in the coordination of OH functionalities brings the ligand L^{4-} in a coplanar disposition to the row of metals.

It is interesting to note that this conversion is related with the formation of a more compact product as can be noticed by a significant increase in the density starting from 2.241 in **3** being 2.343 in **4** and 2.429 in **6**.

As confirmed by PXRD data, **6** was obtained in high yield by direct synthesis from the hydrated gadolinium nitrate and H_4L in 1:1 molar ratio in the presence of 3 equivalents of NaOH in hydrothermal conditions at 160 °C (24 h) or simply from **1** in hydrothermal conditions at 160 °C (24 h).

$$2\ Gd(NO_3)_3 + 2\ H_4L + 7\ H_2O + 6\ NaOH \xrightarrow{H2O} 1/n\ \{[Gd_2(H_2L)(L)(H_2O)_5]\ 2H_2O\}_n + 6\ NaNO_3 \quad (7)$$

6

$$\{[Gd_2(H_2L)_3(DMF)_4]\cdot 2DMF + 7\ H_2O \xrightarrow{H2O} 1/n\ \{[Gd_2(H_2L)(L)(H_2O)_5]\ 2H_2O\}_n + H_4L \quad (8)$$

1 6

The structural characterization of **4** reveals some interesting coordinative and geometrical features. As in **1** and **3** the connector/Gd molar ratio is 1.5 and gadolinium coordination number is 8; in **4** all metal centres exhibit the same coordination geometry. Moreover the connector $[H_2L]^{2-}$ shows in **4** two coordination modes 1a and the new 1f, in which one of the phenolic OH is involved in the coordination to the metal. The gadolinium centre is connected to one phenolic OH and to six different carboxylic groups, one of them is chelate while the other five are shared with two other metal centres. Bridging carboxyl groups form, as in **5** and **6**, rows of metal atoms (Figure 12). The rows run in the *b* direction, which is the elongation axis of the prismatic crystals. Each row is connected by the spacers to six nearest rows (differently from **5** where each row is connected to four adjacent rows) making the 3D network shown in Figure 13. Within the framework, two water molecules are hosted for each gadolinium centre.

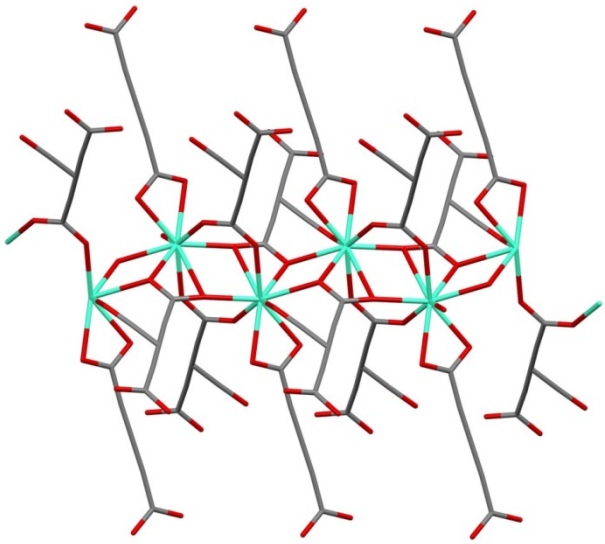

Figure 12. Row of metals running in the *b* direction in the structure of **4**.

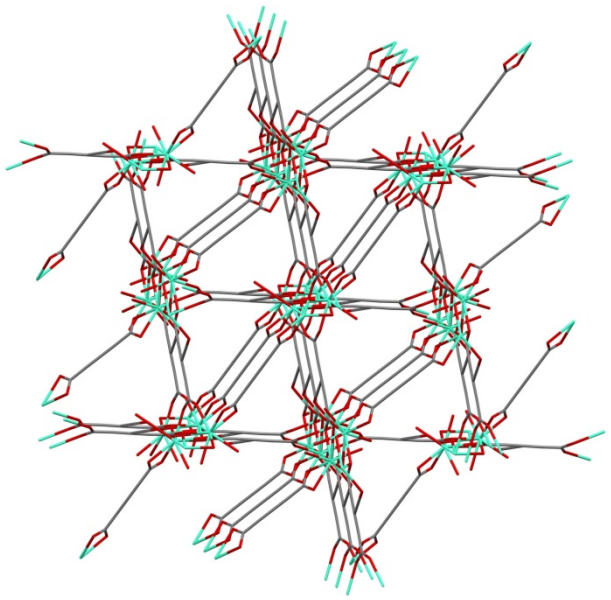

Figure 13. View of the 3D framework in the structure of **4** projected in the *a* direction.

It is reasonable to suppose that this type of coordination can be the first step to the further deprotonation of the connector. In fact a metal coordinated OH will be more acidic than a free one, promoting the proton transfer to an oxygen atom of a carboxylate group. Although the process that move the conversion of **3** to **5** and **6** is difficult to be rationalized in its details, **4** could be an important intermediate.

As discussed in the introduction both $[H_2L]^{2-}$ and $[L]^{4-}$ anions can be generated from H_4L in the course of the syntheses of MOFs based on this connector. For all lanthanide MOFs when the reactions between the metal precursor and H_4L are carried out in DMF containing only minor amounts of water, deprotonation of the connector stops at the dianionic form with formation of $\{[Ln_2(H_2L)_3(DMF)_4]\cdot 2DMF\}_n$. The same outcome was observed even when a large amount of water was present (DMF:H_2O molar ratio about 1:1, 120 °C, 24 h), as reported by Stylianou [6e] and co-workers for the synthesis of $\{[Tb_2(H_2L)_3(DMF)_4]\cdot 2DMF\}_n$. Nevertheless, the authors report that in those conditions, after a prolonged reaction time (72 h), the reaction afforded the derivative $\{[Tb_2(H_2L)(L)(DMF)_2]\}_n$, where a new connector/metal molar ratio is established with the partial deprotonation of $[H_2L]^{2-}$ to $[L]^{4-}$.

$$\{[Tb_2(H_2L)_3(DMF)_4]\cdot 2DMF\}. \rightarrow \{[Tb_2(H_2L)(L)(DMF)_2]\}_n, + H_4L \quad (9)$$

Two points deserve to be underlined: a) in DMF, the evolution to MOF containing $[L]^{4-}$, observed only at high concentration of water, is probably driven by a certain solubility of

$\{[Tb_2(H_2L)_3(DMF)_4]\cdot 2DMF\}_n$ in the reaction medium; b) despite the high water concentration, DMF is preferred to H_2O as additional ligand as well as channel host. The conversion observed in this work shares with the Stylianou's report the evolution to a more stable system with different ligand to metal molar ratio and release of the H_4L ligand. In water **6** appears to be the thermodynamic compound and its formation has probably to rely on a certain solubility of the intermediate phases since the structural differences of **3**, **4**, **5** and **6** make not easy to design a path in the solid state.

Taking into account that water favours the further deprotonation of the connector and that the evolution of **1** to **6** involves the release of H_4L we reckoned that it was possible to convert back **6** to **1** in DMF, containing only minor amounts of water, by addition of the free H_4L acid. The reaction was carried out at 90 °C and the conversion was clearly ascertained by FTIR and PXRD characterizations of the product.

$$\underset{\mathbf{6}}{1/n\ \{[Gd_2(L)(H_2L)(H_2O)_5]\ 2H_2O\}_n} + H_4L + 4\ DMF \rightarrow \underset{\mathbf{1}}{1/n\ \{[Gd_2(H_2L)_3(DMF)_4]\cdot 2DMF\}_n} + 7\ H_2O \qquad \mathbf{10}$$

Therefore, **1** and **6** appear to be interconnected in a way strongly dependent on the solvent nature as well as on the temperature. In the course of the treatment of **6** with H_4L in DMF, H_2O is substituted by DMF and the Gd:L molar ratio is reverted to 2:3 with formation of **1**. In absence of free H_4L no transformation was observed in those conditions, also for long reaction times ruling out the possibility of redistribution of the ligand, for example into **1** and the hypothetical $[Gd_4(L)_3(DMF)_x]\cdot y$DMF (Eq.11).

$$\underset{\mathbf{6}}{3/n\ \{[Gd_2(L)(H_2L)(H_2O)_5]\ 2H_2O\}_n} + (6+x+y)\ DMF \rightarrow$$
$$\rightarrow \underset{\mathbf{1}}{1/n\ \{[Gd_2(H_2L)_3(DMF)_4]\cdot 2DMF\}_n} + 1/n\ \{[Gd_4(L)_3(DMF)_x]\cdot yDMF\}_n\ 21\ H_2O \qquad (11)$$

On the other hand, the conversion of **1** to **6** as well as the one of **3** to **6** in water entails the release of H_4L. In the scheme below, a summary of the transformations we have examined is depicted together with the conditions required to drive the system in the various directions.

Water as solvent at about 160 °C moves the species with composition $[Ln_2(H_2L)_3]$ to release H_4L with evolution to $[Ln_2(H_2L)(L)]$, while in DMF at about 90 °C the process is reversed.

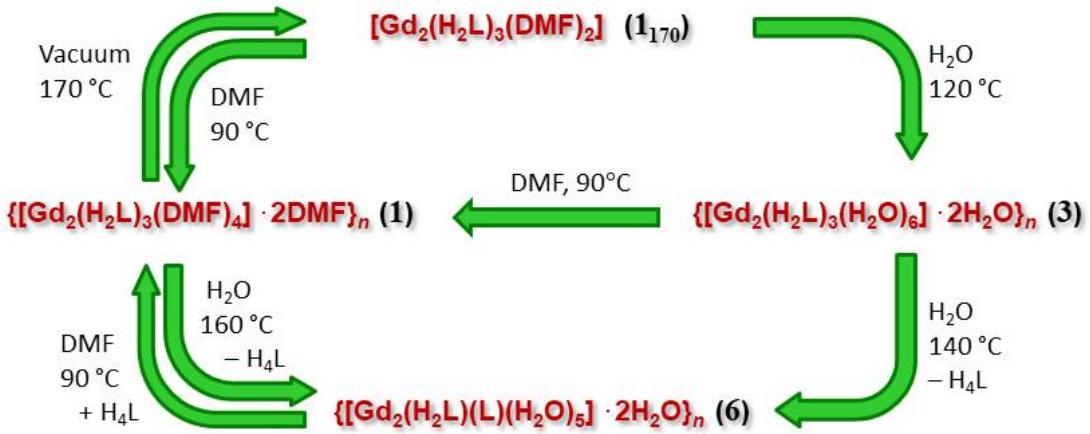

4. Conclusions

Access to different lanthanide MOFs based on H_4L, potential precursor of H_2L^{2-} and (L^{4-}) anions, has been established. Both solvent identity and temperature influence the outcome of the processes. Syntheses carried out in DMF with a Gd/H_4L molar ratio 2:3 at 90 °C yielded product **1**, with unreacted phenolic functionalities. The low solubility of **1** in hot anhydrous DMF avoids further modifications. On the other hand the reaction carried out in H_2O with the same Gd/H_4L molar ratio produces in controlled conditions the hydrated derivative **3,** as a single product. This compound, having unreacted phenolic functionalities reacting further is transformed into **4** (same metal/ligand molar ratio), via an initial interaction of some phenolic oxygen atoms with the metals, and successively into the derivatives $Gd_2(H_2L)_2(L)_{0.5}$, **5**, and $Gd_2(H_2L)(L)$, **6**, where partial deprotonation of the phenolic functionalities progressively modifies the ligand to metal molar ratio. Anyway, a solid state transition appears not practicable, since the described MOFs are quite different structurally so that a dissolution-recrystallization process is likely. In water, the prevailing product of the resulting solid mixtures appears to be dependent on the temperature and time of the process, with product **6** being the final product that can be recovered analytically pure. **1** and **6** can be interconverted with loss or addition of H_4L in the appropriate conditions where, besides the

temperature, the solvent plays an important role. Although different MOFs can be obtained from the same precursors, the conditions for high yield syntheses of pure **1**, **2**, **3** and **6** have been determined. The assemblage of ligands and metal ions to obtain MOFs can produce derivatives with different composition and/or structure. The knowledge of the parameters influencing the process outcome and the way they act is an important task to control the targeted production of these interesting functional materials.

Acknowledgments The authors wish to thank Ministero Istruzione Università e Ricerca, MIUR (PRIN 2015, 20154X9ATP, Progetti di Ricerca di Interesse Nazionale) and PRA_2018_23 Materiali Funzionali, Progetti di Ricerca di Ateneo) for financial support.

References

[1] (a) K. Sumida, D. L. Rogow, J. A. Mason, T. M. Mc Donald, E. D. Bloch, Z. R. Herm, T. -H. Bae, J. R. Long, Chem. Rev., 112 (2011) 724–781; (b) M. P. Suh, H. J. Park, T. K. Prasad, D. -W. Lim, Chem. Rev., 112 (2011) 782–835; (c) S. Lee, E. A. Kapustin, O.M. Yaghi, Science, 353 (2016) 808–811; (d) S. Kitagawa, Acc. Chem. Res., 50 (2017) 514–516; (e) H. Kim, S. Yang, S. R. Rao, S. Narayanan, E. A. Kapustin, H. Furukawa, A.S. Umans, O.M. Yaghi, E.N. Wang, Science, 356 (2017) 430–434; (f) Y. Cui, Y. Yue, G. Qian, B. Chen, Chem. Rev., 112 (2011) 1126–1162; (g) Y. Cui, B. Chen, G. Qian, Coord. Chem. Rev., 273 (2014) 76–86; (h) M. D. Allendorf, C. A. Bauer, R. K. Bhakta, R. J. T. Houk, Chem. Soc. Rev., 38 (2009) 1330−1352; (i) J. Rocha, L. D. Carlos, F. A. A. Paz, D. Ananias, Chem. Soc. Rev., 40 (2011) 926−940; (l) X. Cui, K. Chen, H. Xing, Q. Yang, R. Krishna, Z. Bao, H. Wu, W. Zhou, X. Dong. Y. Han, B. Li, Q. Ren, M. J. Zaworotko, B. Chen, Science, 353 (2016) 141–144; (m) A. Cadiau, K. Adil, P. M. Bhatt, Y. Belmabkhout, M. Eddaoudi, Science, 353 (2016) 137–140.

[2] (a) J. S. Seo, D. Whang, H. Lee, S. I. Jun, J. Oh, Y. J. Jeon, K. Kim, Nature, 404 (2000) 982-986; (2b) B. Chen, M. Eddaoudi, S. T. Hyde, M. O'Keeffe, O. M. Yaghi, Science, 291 (2001) 1021-1023; (2c) O. Sato, T. Iyoda, A. Fujishima, K. Hashimoto, Science, 271 (1996) 49-51; (d) O. Kahn, C. Martinez, Science, 279 (1998) 44-48.

[3] S. M. Cohen, Chem. Rev., 112 (2012) 970–1000.

[4] (a) C. D. Ene, F. Tuna, O. Fabelo, C. Ruiz-Perez, A. M. Madalan, H. W. Roesky, M. Andruh, Polyhedron 27 (2008) 574-582; (b) M. Eddaoudi, J. Kim, N. Rosi, D. Vodak, J. Wachter, M. O'Keeffe, O. M. Yaghi, Science 295 (2002) 469-472; (c) N. L. Rosi, J. Kim, M. Eddaoudi, B. Chen, M. O'Keeffe, O. M. Yaghi, J. Am. Chem. Soc., 127 (2005) 1504-1518; (d) P. D. C. Dietzel, R. Blom, H. Fjellvag, Dalton Trans., (2006) 2055-2057; (e) P. D. C. Dietzel, B. Panella, M. Hirscher, R. Blom, H. Fjellvag, Chem. Commun., (2006) 959-961; (f) P. D. C. Dietzel; Y. Morita, R. Blom, H. Fjellvag, Angew. Chem., Int. Ed., 44 (2005) 6354-6358; (g) P. D. C. Dietzel, R. E. Johnsen, R. Blom, H. Fjellvag, Chem. Eur. J., 14 (2008) 2389-2397; (h) N. E. Ghermani, G. Morgant, J. d'Angelo, D. Desmaele, B. Fraisse, F. Bonhomme, E. Dichi, M. Sgahier, Polyhedron 26 (2007) 2880-2884; (i) J. F. Bickley, R. P. Bonar-Law, C. Femoni, E. J. MacLean, A. Steinera, S. J. Teat, J. Chem. Soc., Dalton Trans., (2000) 4025-4027.

[5] (a) R. W. Corkery, Curr. Opin. Colloid Interface Sci., 13 (2008) 288−302; (b) Y. Cui, B. Chen, G. Qian, Coord. Chem. Rev., 273-274 (2014) 76−86; (c) Y. Cui, B. Chen, G. Qian, Struct. Bonding, 157 (2013) 27−88; (d) S. Fordham, X. Wang, M. Bosch, H.-C. Zhou, Struct. Bonding 163 (2014) 1−27; (e) B. Li, B. Chen, Struct. Bonding, 163 (2014) 75−107; (f) L. Ma, W. Lin, Top. Curr. Chem., 293 (2009) 175−205; (g) X. Zhang, W. Wang, Z. Hu, G. Wang, K. Uvdal, Coord. Chem. Rev., 284 (2015) 206−235; (h) Z. Zhang, Z. Zheng, Struct. Bonding, 163 (2014) 297−367.

[6] (a) S. Nayak, H. P. Nayek, C. Pietzonka, G. Novitchi, S. Dehnen, J. Mol. Struct., 1004 (2011) 82–87; (b) Y.-L. Wang, Y.-L. Jiang, Q.-Y. Liu, Y.-X. Tan, J.-J. Wei, J. Zhang, CrystEngComm, 13 (2011) 4981–4987; (c) K. L. Gurunatha, S. Mohapatra, P. A. Suchetan, T. K. Maji, Cryst.Growth Des., 9 (2009) 3844-3847; (d) Y.-L. Wang, Y.-L. Jiang, Z.-J. Xiahou, J.-H. Fu, Q.-Y. Liu, Dalton Trans., 41 (2012) 11428-11437; (e) S. L. Anderson, A. Gładysiak, P. G. Boyd, C. P. Ireland, P. Miéville, D. Tiana, B. Vlaisavljevich, P. Schouwink, W. van Beek, K. J. Gagnon, B. Smit, K. C. Stylianou, CrystEngComm., 19 (2017) 3407–3412.

[7] N. L. Rosi, M. Eddaoudi, J. Kim, M. O'Keeffe, O. M. Yaghi, CrystEngComm, 4 (2002) 401–404.

[8] V. S. Sastri, J.-C. G. Bünzli, R. V. Rao, G. V. S. Rayudu, J. R. Perumareddi, "Modern Aspects of Rare Earths and Their Complexes" (2003) 262-263, Elsevier.

[9] I. M. Kolthoff, P. J. Elving, "Treatise on Analytical Chemistry" 8 (1963) 54, Interscience-Wiley, NY.

[10] A. Jerschow, N. Müller, J. Magn. Reson., 125 (1997) 372–375.

[11] R. Mills, J. Phys. Chem., 77 (1973) 685-688.

[12] (a) E. O. Stejskal, J. E. Tanner, J. Chem. Phys., 42 (1965) 288-292; (b) A. Macchioni, G. Ciancaleoni, C. Zuccaccia, D. Zuccaccia, Chem. Soc. Rev., 37 (2008) 479-489.

[13] (a) L. Armelao, D. Belli Dell'Amico, P. Biagini, G. Bottaro, S. Chiaberge, P. Falvo, L. Labella, F. Marchetti, S. Samaritani Inorg. Chem., 53 (2014) 4861-4871; (b) D. Belli Dell'Amico, M. De Sanctis, R. Ishak, S. Dolci, L. Labella, M. Lezzerini, F. Marchetti, Polyhedron, 99 (2015) 170-176; (c) D. Belli Dell'Amico, P. Biagini, S. Chiaberge, L. Falchi, L. Labella, M. Lezzerini, F. Marchetti, S. Samaritani, Polyhedron, 102 (2015) 452-461; (d) D. Belli Dell'Amico, A. Di Giacomo, C. Evangelisti, L. Falchi, L. Labella, M. Marelli, M. Lezzerini, F. Marchetti, S. Samaritani, Polyhedron, 123 (2017) 33-38; (e) D. Belli Dell'Amico, P. Biagini, G. Bongiovanni, S. Chiaberge, A. Di Giacomo, L. Labella, F. Marchetti, G. Marra, A. Mura, F. Quochi, S. Samaritani, V. Sarritzu, Inorg. Chim. Acta, 470 (2018) 149-157; (f) D. Belli Dell' Amico, F. Calderazzo, S. Farnocchi, L. Labella, F. Marchetti, Inorg. Chem. Commun., 5 (2002) 848-852.

[14] G. M. Sheldrick, Acta Crystallogr., Sect. A: Found. Crystallogr., 64 (2008) 112-122.

[15] (a) W. Armarego, C. Chau, "Purification Of Laboratory Chemicals," Butterworth-Heinemann 6th Ed, 2009; (b) J. Muzart, Tetrahedron, 65 (2009) 8313-8323. (c) W. Liu, C. Chen, H. Liu, Beilstein, J. Org. Chem, 11 (2015) 1721–1726.

[16] D. J. Tranchemontagne, J. R. Hunt, O. M. Yaghi, Tetrahedron, 64 (2008) 8553–8557.

[17] (a) L. Armelao, D. Belli Dell'Amico, L. Bellucci, G. Bottaro, L. Labella, F. Marchetti, S. Samaritani Inorg. Chem., 55 (2016) 939-947; (b) L. Armelao, D. Belli Dell'Amico, L. Bellucci, G. Bottaro, L. Di Bari, L. Labella, F. Marchetti, S. Samaritani, F. Zinna, Inorg. Chem., 56 (2017) 7010-7018; (c) L. Armelao, D. Belli Dell'Amico, G. Bottaro, P. Falvo, L. Labella, F. Marchetti, D. Parisi, S. Samaritani, Polyhedron, 85 (2015) 770-776.